World Conference on Timber Engineering 2021

WCTE 2021
WORLD CONFERENCE ON TIMBER ENGINEERING
SANTIAGO, CHILE | 9 - 12 AUGUST

Centro UC de Innovación en Madera
MADERA21 de CORMA

Santiago, Chile 2021 / Conference Proceedings

World Conference on Timber Engineering (WCTE 2021)

Santiago, Chile
9-12 August 2021

ISBN(PDF): 978-1-7138-4111-1
ISBN(Print): 978-1-7138-4097-8

Produced with permission by:

Curran Associates, Inc.
57 Morehouse Lane
Red Hook, NY 12571

World Conference on Timber Engineering 2021 (WCTE'21)

https://wcte2021.com/

Additional copies of this publication are available from:

Curran Associates, Inc.
57 Morehouse Lane
Red Hook, NY 12571 USA
Phone: 845-758-0400
Fax: 845-758-2633
Email: curran@proceedings.com
Web: www.proceedings.com

World Conference on Timber Engineering 2021 Book of Abstracs

Book Photo Cover
Isadora Toledo
Book Design
Constanza Rojas
Content and Translations
Valentina Gutiérrez
Amanda Apurahal

WCTE 2021
WORLD CONFERENCE ON TIMBER ENGINEERING
SANTIAGO, CHILE | 9 - 12 AUGUST

EXPERIMENTAL ESTIMATION OF EQUIVALENT VISCOUS DAMPING FOR POST-TENSIONED TIMBER FRAMED BUILDINGS WITH DISSIPATIVE BRACING SYSTEMS

Antonio Di Cesare[1], Felice Carlo Ponzo[1], Nicla Lamarucciola[1], Domenico Nigro[1]

ABSTRACT: A reliable estimation of the equivalent viscous damping can have a significant impact in displacement-based design procedure. Although the performance-based seismic design approach is advanced for some types of buildings (e.g. reinforced concrete structures), its application to other types structures, such as post-tensioned timber framed buildings with dissipative bracing systems, still requires further investigation. In this paper the equivalent viscous damping of a three-dimensional, three storey, 2/3 scaled, post-tensioned timber framed structure, with and without V-inverted dissipative bracing systems, is estimated from shaking table tests considering an approach based on the equality of the dissipated energy with stored one. The experimental results are compared with numerical non-linear time history analyses and with formulations available in literature.

KEYWORDS: Displacement-based design, post-tensioned timber frame, dissipative bracing systems, shaking table tests, equivalent viscous damping

1 INTRODUCTION

In a severe seismic motion, most structure are designed to preserve lives dissipating the energy of the earthquake through structural damages, which can led to high loss of functionality and the building may be unusable after the event [1].

The concept of viscous damping is generally used to represent various mechanisms of energy dissipation of the structure (such as cracking, nonlinearity in the elastic phase of response, interaction with non-structural elements, soil-structure interaction, etc.). There is no direct relationship of such damping with the real physical phenomena, however the adoption of the viscous damping concept facilitates the solution of the differential equation of motion.

The equivalent damping approach was first proposed by Jacobsen in 1930 [2], suggesting an approximate solution of the steady-state response of a nonlinear oscillator by defining an equivalent linear oscillator with the same natural frequency and dissipating equal energy per cycle of sinusoidal response. In 1960 Jacobsen [3] proposed the estimation of the hysteretic equivalent viscous damping of building structures producing large deflections beyond its elastic limit, by equating the energy absorbed by hysteretic cyclic response at a given displacement amplitude to the equivalent viscous damping of the SDOF system, considering a sinusoidal response to ensure complete loops. Experimental hysteretic responses and idealized construction were used to estimate the damping of composite structures based on the concept of dissipated (E_{Diss}) and stored (E_{sto}) energy as shown in Figure 1. The following Equation (1) was proposed, where A_{hyst} represents the area of dissipated energy, F_0 and u_0 are the maximum force and displacement for the given hysteretic loop.

$$\xi_{hyst} = \frac{1}{4\pi}\frac{E_{diss}}{E_{sto}} = \frac{1}{2\pi}\frac{A_{hyst}}{F_0 u_0} \quad (1)$$

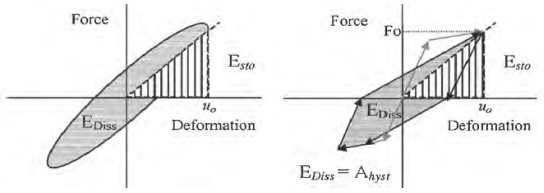

***Figure 1**: Dissipated and stored force for viscous damping and hysteretic cycles (Jacobsen's formulation)*

It is worth noting that there are many difficulties in the prediction of effective damping of building during a strong motion earthquake, due to the random excitation

[1] Antonio Di Cesare, School of Engineering University of Basilicata, Italy, antonio.dicesare@unibas.it
Felice Carlo Ponzo, School of Engineering University of Basilicata, Italy, felice.ponzo@unibas.it
Nicla Lamarucciola, School of Engineering University of Basilicata, Italy, nicla.lamarucciola@unibas.it
Domenico Nigro, School of Engineering University of Basilicata, Italy, domenico.nigro@unibas.it

and to the observation that the complete loops are not formed in each cycle.

Based on this initial formulation, the equivalent damping was investigated by several authors. Rosenblueth and Herrera (1964) [4] developed the equivalent damping expression as a function of ductility (μ) and post-yielding stiffness ratio (r), based on secant stiffness, at the maximum displacement by considering the period shift between the original and equivalent systems. Extending the work of Jacobsen (1960), Gulkan and Sozen (1974) [5] applied the concept of substitute damping to approximate the inelastic behavior of a SDOF reinforced concrete (RC) frames utilizing energy balance to obtain equivalent damping values for Takeda model. Iwan (1980) [6] proposed an expression of equivalent viscous damping for elastic coulomb and slip elements. Chopra (1995) [7] estimated the elastic viscous damping measuring the amplitude decay from experimental tests in laboratories or real buildings. In practice, for r.c buildings the value of the coefficient ranges between 2% and 5%. The study by Dwairi et al. (2007) [8] used a large number of real accelerograms to calibrate the equivalent viscous damping, providing a relationship for a given rule, ductility and period. Dwairi proposed a hyperbolic damping ductility law based on nonlinear ductility at peak displacement for unbounded post-tensioned concrete systems, RC beams, RC columns and steel members. Filialtraut (2003) [9] estimated the equivalent damping variation of wood framed buildings with displacement amplitude. Blandon and Priestley (2005) [10] compared the EVD based on Jacobsen's approach and EVD from the iterative time history analyses for six different hysteretic models. They concluded that Jacobsen's approach overestimated EVD values; thus, they proposed corrected equations for the DBD method. Priestley and Grant (2005) [11] proposed the equivalent damping for different hysteretic model as a function of the ductility (μ), the post-yield stiffness ratio (r), and the re-centering ratio of the global system (β_F), for the flag-shape model Figure 2b). Pennucci et al. (2009) [12] proposed an equivalent viscous damping equation for flag-shaped hybrid systems as a function of λ (related to the flag loop parameter as the ratio between the amount of post-tensioning and the amount of dissipation). An equivalent viscous damping-ductility law for various post-yield stiffness ratios, valid for steel members, was defined by Bezabeh et al. (2016) [13] considering a series of non-linear time histories analyses.

The results of some of these studies are summarized in

Equation (2) shows the total equivalent damping ξ_{eq} of the SDOF system as reported in Priestley et al. [14]:

$$\xi_{eq} = \xi_0 + \xi_{hyst} \quad (2)$$

where ξ_0 is the elastic viscous damping and ξ_{hyst} is related to the inelastic hysteresis. Priestley et al. [14] suggested that the hysteretic damping value should be corrected by a dynamic reduction factor k to obtain hysteretic damping that is consistent with the results of inelastic time history analysis Equation (3), in order to account for the random nature of seismic inputs.

$$\xi_{eq} = \xi_0 + k\xi_{hyst} \quad (3)$$

A reliable estimation of the equivalent viscous damping plays a fundamental role in Displacement Based Design (DBD) procedure [14] for a correct design of the structural system. The base concept of DBD (Figure 2) consist in the approximation of a multi-degree of freedom (MDOF) structure with a single degree of freedom (SDOF) system with effective mass (m_e), equivalent secant stiffness (K_e) and period (T_e), and equivalent viscous damping (ξ_{eq}) at target design displacement (Δ_d) or drift (θ_d). The maximum displacement and base shear (F_u) of the SDOF system will be approximately equal to the original MDOF structural response. It allows to consider the energy dissipation due to the non-linear behaviour by reducing the linear response spectrum. In this way it is possible to solve a simple linear system instead of a non-linear system with reduced time and resource demanding.

Table 1: *Existing equivalent viscous damping equations.*

Structural system	*Researcher*	*Equation*
Bilinear elasto-plastic systems	Rosenblueth and Herrera (1964)	$\xi_{eq} = \xi_0 + \frac{2}{\pi}\left[\frac{(1-r)(\mu-1)}{\mu - r\pi + r\mu^2}\right]$
Takeda model	Gulak and Sozen (1974)	$\xi_{eq} = \xi_0 + 0.2\left(1 - \frac{1}{\sqrt{\mu}}\right)$
Elastic and Coulomb slip elements	Iwan (1980)	$\xi_{eq} = \xi_0 + 0.0587(\mu-1)^{0.371}$
Wood framed buildings	Filialtraut (2003)	$\xi_{eq} = \begin{cases} 0.5\Delta_b + 0.02 & 0 \le \Delta_b \le 0.36\% \\ 0.2 & \Delta_b > 0.36\% \end{cases}$
RC flag-shaped hysteretic systems	Priestley and Grant (2005)	$\xi_{eq} = \xi_0 + k\frac{\beta_F(\mu-1)}{\mu\pi[1+r(\mu-1)]}$
	Dwairi (2007)	$\xi_{eq} = \xi_0 + C\left(\frac{\mu-1}{\mu\pi}\right)$ $C = 30 + 35(1-T_e) \quad T_e < 1sec$ $C = 30 \quad T_e > 1sec$
	Pennucci et al. (2009)	$\xi_{eq} = \xi_0 + k\frac{2}{(\lambda+1)}\left(\frac{\mu-1}{\mu\pi}\right)$

In order to significantly reduce structural and non-structural damage and avoid high economic loss, the number of applications of low-damage structures, in which the damping is concentrated into replaceable anti-seismic dissipative devices [15],[16], is rapidly increasing.

Recently, pre-stressed laminated (Pres-Lam) timber buildings are emerging and several applications have been registered in New Zealand and throughout the world, particularly in seismic areas. This technique is based on the PRESSS system, originally developed for precast concrete frame and wall construction [17], and consists in the use of high strength unbounded steel cables or bars to create connections between timber beams and columns, or between columns and walls and their foundations.

Several studies and experimental applications [18]-[20] have been performed considering additional dissipative dampers, to provide additional strength and energy dissipation capability and creating a damage-avoiding structural system.

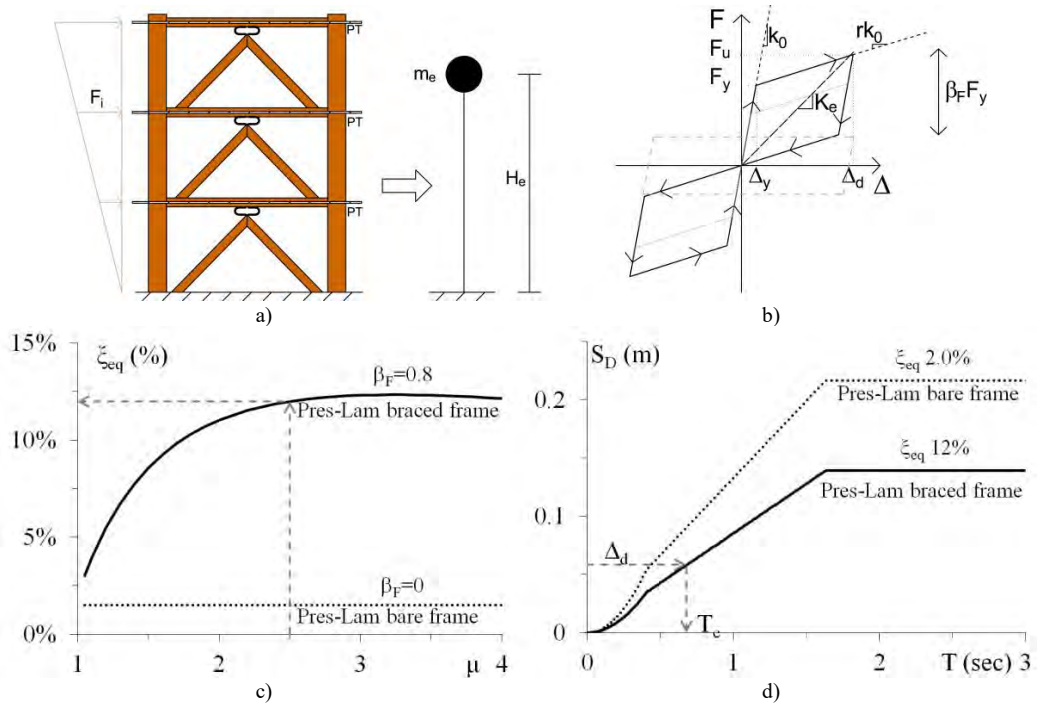

Figure 2: *Basics of DBD approach: (a) SDOF representation; (b) effective stiffness of a flag-shaped system; (c) equivalent viscous damping versus ductility; (d) design displacement spectra*

The introduction of metallic yielding dampers represents an optimal low-cost solution requiring a little maintenance and easily replaceable in case of damage. Hysteretic dampers are independent of temperature and velocity of motion and generally are manufactured by traditional materials.

In this paper a three-dimensional post-tensioned timber frame prototype was designed and tested on the shaking table available at the structural laboratory of the University of Basilicata considering various configurations with and without dissipative bracing systems. The design of the model was based on the DBD procedure, optimized for Pres-Lam buildings with dissipative systems as reported in Di Cesare et al. [21], [22]. The equivalent damping equation proposed by Priestley and Grant [11] for unbounded post-tensioned systems (flag-shape model) was used in the design procedure.

In order to validate the reliability of the equivalent damping considered in the design procedure, the results of the shaking table tests were compared with the corresponding design values and with the results of non-linear dynamic analyses.

The motivation of the present study is the experimental estimation of the equivalent viscous damping of post-tensioned timber framed buildings with dissipative bracing systems.

2 EXPERIMENTAL TESTING

A 3D, 2/3 scaled Pres-Lam experimental model with three stories (inter-storey height of 2 m) and a single bay in both directions with a footprint of 3m x 4m was designed and tested at the structural laboratory of the University of Basilicata [21],[22]. The prototype model was post-tensioned in both directions at 100 kN and 50 kN in the longitudinal and transversal directions, respectively. The frame was designed according to Eurocode for office utilization at the first and second levels ($Q = 3$ kN/m^2) and as rooftop garden at the third level ($Q = 2$ kN/m^2). The flooring panels spanned in both directions have been made by a series of deep glulam beams turned on their sides. Appropriate scaling factors were applied according to the Cauchy-Froude similitude laws to evaluate the additional masses on the structure [23]. The prototype model was tested in different configurations with and without energy dissipation systems, for more detail about the experimental campaign please refer to Di Cesare et al. [24].

This paper describes the experimental shaking table tests performed on the post-tensioned timber frame with dissipative braces [22], as shown in Figure 3. The dissipative braced frame model was designed at target drift of 1.25% and a flag loop parameter $\beta_F = 0.8$, with a total equivalent viscous damping of $\xi_{eq} = 12\%$, by applying the equation proposed by Priestley and Grant

(2005) [11] with k=0.85. The main design parameter and the results obtained by the DBD procedure is summarized in Table 2.
From the flag-shape behavior, the characteristics of the equivalent bare frame and of the equivalent dissipative bracing system were obtained [22]. Each dissipative brace was composed by two 160 mm x 180 mm V-inverted timber rods and a couple of C60 steel grade U-shaped flexural plates (UFP) dampers with different geometrical dimensions at each storey, working in parallel.
.

Figure 3: *Experimental post-tensioned timber frame model tested at the structural laboratory of University of Basilicata.*

Table 2: *Main design parameters of DBD procedure for the braced model.*

Design parameter	BF config.
θ_d	1.25%
β_F	0.8
μ	2.5
r	0.2
$\xi_{eq,v}$	2%
ξ_{eq}	12%
m_e	14.4 t
T_e	0.68 s
K_e	1228 kN/m
F_u	71 kN

In Table 3 the main mechanical characteristics of UFPs installed to each storey of the bracing system are summarized.

Table 3: *Main characteristics of UFP dampers*

Level	damper ID	b_u (mm)	t_u (mm)	D_u (mm)
1st storey	UFP1	60		
2nd storey	UFP2	40	6	60
3rd storey	UFP3	30		

Figure 4 shows the construction details between the dissipative bracing connection and beam, a detail of UFP1 damper and corresponding the force-displacement behaviour obtained during preliminary quasi-static characterization tests [23] performed at the structural laboratory of University of Basilicata. More detailed information about the design procedure and connection details can be found in Di Cesare et al.[26].

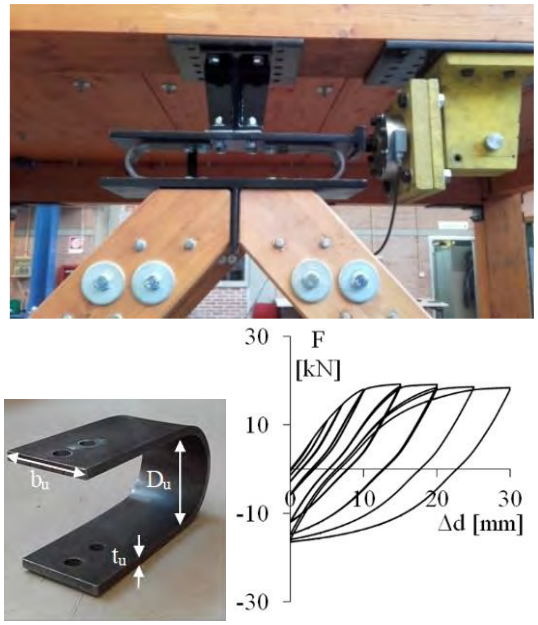

Figure 4: *Construction detail between the dissipative bracing and beam, detail of UFP1 and constitutive law.*

Seven different spectra-compatible natural earthquakes at increasing PGA intensities were selected from the European Strong motion database. The design spectrum was defined considering a peak ground acceleration PGA of 0.44 g and medium soil class according to Eurocode for high seismic zone. In this paper a reduced set of three spectra-compatible earthquake has been considered, as shown in Figure 5.
The shake table testing program of the post-tensioned timber braced model for the three selected seismic inputs considered in this paper is summarized in Table 4.
The global and local dynamic response of the experimental frame was recorded in real time by 54 sensors consisting of horizontal and vertical accelerometers, displacement transducers, potentiometers and load cells.

ID Code	Location	Date	M_W	PGA (g)	Scale Factor
1228	Izmit, Turkey	17/08/1999	7.6	0.357	1.5
196	Montenegro Serbia	15/04/1979	6.9	0.454	1
535	Erzican Turkey	13/03/1992	6.6	0.769	1.5

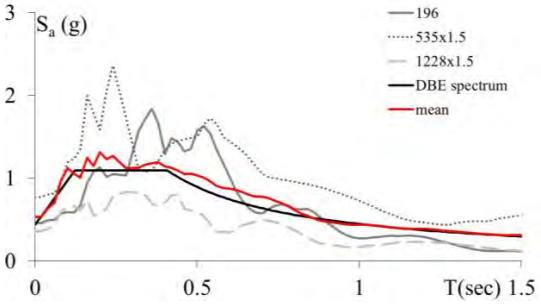

Figure 5: *Seismic inputs selected for shaking table tests.*

Table 4: *Testing program for selected earthquakes*

PGA	*Seismic inputs*		
	1228	*196*	*535*
10%	x	x	x
25%	x	x	x
50%	x	x	x
75%	x	x	x
100%	x	x	x

3 EXPERIMENTAL AND NUMERICAL RESULTS

The numerical model of the test frame with dissipative bracing systems was implemented in SAP2000 [27] using a lumped plasticity approach, which combines the use of elastic elements with linear or rotational springs representing plastic deformations of the system. A 2D finite elements frame-type was used to model the braced frame as shown in Figure 6. The structural elements (beams, columns and braces) were modelled as elastic elements with anisotropic glulam timber material. The connection between beam and column was modelled with a combination of rotational springs to represent the contribution of the post-tensioning (multi-linear elastic link) and the flexibility of the joint panel (linear elastic link). The column base connection was modelled with 3 rotational springs in parallel, which considered the moment resistance given by the contribution of the gravity plus seismic axial load and the additional moment contribution of hysteretic steel elements [28]. Finally, the nonlinear force-displacement hysteretic behaviour of the UFP dampers was modelled by using link elements connecting the elastic beam and V-inverted braces [29], characterized by the Bouc-Wen cyclic laws [30], [31]. The constitutive laws of rotational springs and nonlinear links are represented in Figure 6.

Viscous proportional damping is specified for direct-integration time-history analyses of the timber frame. In this paper non-linear dynamic analyses of the numerical model have been performed for earthquakes 1228, 196 and 535 at all PGA levels.

Figure 7 shows the comparison between numerical and experimental results in terms of mean value of maximum displacements recorded at the third storey for the three seismic inputs at all PGA levels. As can be observed, the numerical results are in good agreement with experimental values showing a linear increasing trend at growing PGA levels. Maximum values of 86 mm and 82 mm for experimental and numerical outcomes were recorded.

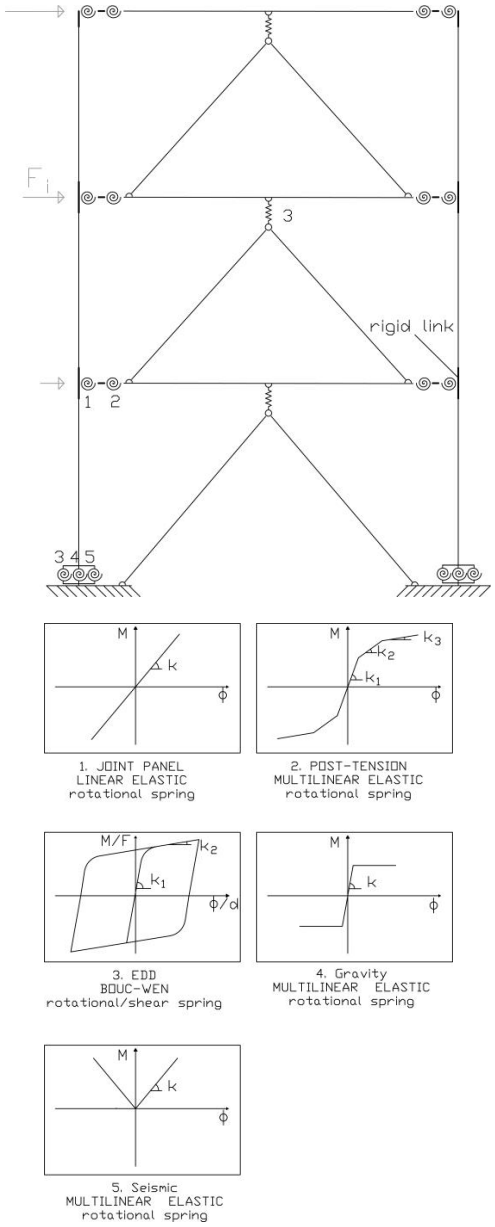

Figure 6: *2-D numerical model of the braced frame and constitutive laws of elements connections.*

The comparison between the experimental and numerical seismic response of the braced post-tensioned frame is shown in Figure 8 and Figure 9 in terms of global and local behaviour for the three earthquake inputs 1228, 196 and 535 at 25%, 75% and 100% of PGA levels.
Figure 8 shows the global hysteretic response in terms of base shear and lateral top displacement. As can be observed the experimental and numerical results are in good agreement for all seismic inputs. At 25% of PGA the response of the frame was substantially elastic while the global flag shape loop was more evident at higher PGA levels.

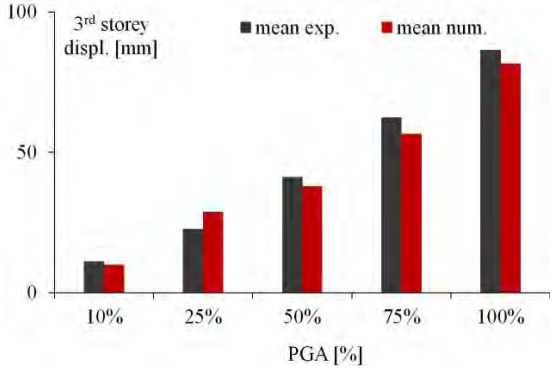

Figure 7: *Comparison between mean numerical and experimental results of 3rd storey displacement for all PGA levels.*

Figure 9 shows the local response in terms of force-displacement of the UFP dampers at the first storey of the bracing system. According to numerical modelling of the braced frame the yield and maximum displacements compared well both for global flag-shape and local hysteresis of dampers. The results of the local response confirmed that the dampers were fully activated at higher PGA levels. A stable hysteretic behaviour and large hysteresis loop were observed for stronger earthquakes 535 and 196, with high amount of energy dissipated.

4 DAMPING ESTIMATION

The equivalent viscous damping has been experimentally estimated as sum of the elastic and hysteretic damping contributions [14] and numerically verified as reported in the following Equation (4):

$$\xi_{eq} = \frac{\delta}{\sqrt{\delta^2 + 4\pi^2}} + k\,\frac{1}{2\pi}\frac{A_{hyst}}{F_0 u_0} \qquad (4)$$

The first contribution of Equation 4 represents the elastic damping of the structural system. It was estimated from experimental and numerical time-domain free vibration response of displacement of the bare post-tensioned frame. Figure 10 shows the reference earthquake input 1228 at 100% of PGA level and the time history of the recorded top displacement compared with the numerical outcome. As can be observed, experimental and numerical results were in good agreement. The free vibration response highlighted in the graph was shown in detail in Figure 11 and based on the measured peak displacement amplitudes of successive cycles, the logarithmic decrement δ [32] was used to find the experimental and numerical elastic damping. It was estimated by averaging many cases of elastic damping (first member of Equation 4) for all successive peaks of the free vibration time history.
As shown in Figure 11 the time-displacement free vibration response was in line with the exponentially narrowing curve (dashed line), related to a value of elastic damping ξ_0 = 2.5%. The same value was estimated by using free vibrations of displacement time histories of the post-tensioned model with dissipative bracing systems. This result highlighted that during free oscillations the dissipative dampers are not activated and the frame responded elastically.
The second contribution of Equation 4 represents the hysteretic damping of the braced frame based on the Jacobsen's formulation [3], multiplied by the dynamic reduction factor k=0.85 [22]. Starting from the global flag-shape hysteretic experimental and numerical responses of the braced model (Figure 8), the hysteretic area A_{hyst} and related maximum force F_0 and displacement u_0 were evaluated for the three seismic input at all PGA levels and the hysteretic equivalent damping was estimated.
Figure 12 shows the comparison between experimental and numerical estimation of equivalent damping (ξ_{eq}) in terms of mean value obtained for the three seismic inputs at increasing PGA levels. As can be observed, the equivalent damping grows at increasing PGA levels and a good agreement between numerical and experimental results was observed. At PGA values higher than 50%, when dissipative dampers were activated, the experimental estimated damping was stable around 14% and around 13% for the numerical model. The design value of equivalent damping ξ_{eq}=12% was in line with the experimental and numerical results.
Figure 13 shows the equivalent damping versus ductility formulations available in literature proposed by some notable authors ([5], [6], [8], [11], [12]) for different structural systems compared with the experimental estimations of equivalent damping and corresponding ductility obtained for the three seismic inputs considered in this study at all PGA levels.
Ductility of experimental models was calculated from global hysteresis responses as the ratio between the ultimate displacement (Figure 8) and the displacement corresponding to the yield point on the idealized response curve. In the current study a maximum value of equivalent damping in the range of 11–16% for ductility values in the range of 3-5 at 100% of PGA was obtained.
As can be observed the experimental results are in line with the formulation of Pennucci et al. (2009) applied to the design flag-shape system (λ=2.23) and with that used in the design procedure due to Priestley and Grant (2005) introducing the reduction factor k=0.85. The formulations proposed by Gulak and Sozen for Takeda model, Iwan for Elastic and Coulomb slip elements and Dwairi for RC flag-shaped hysteretic systems are similar, and the experimental results slightly overestimate the damping-ductility curves.

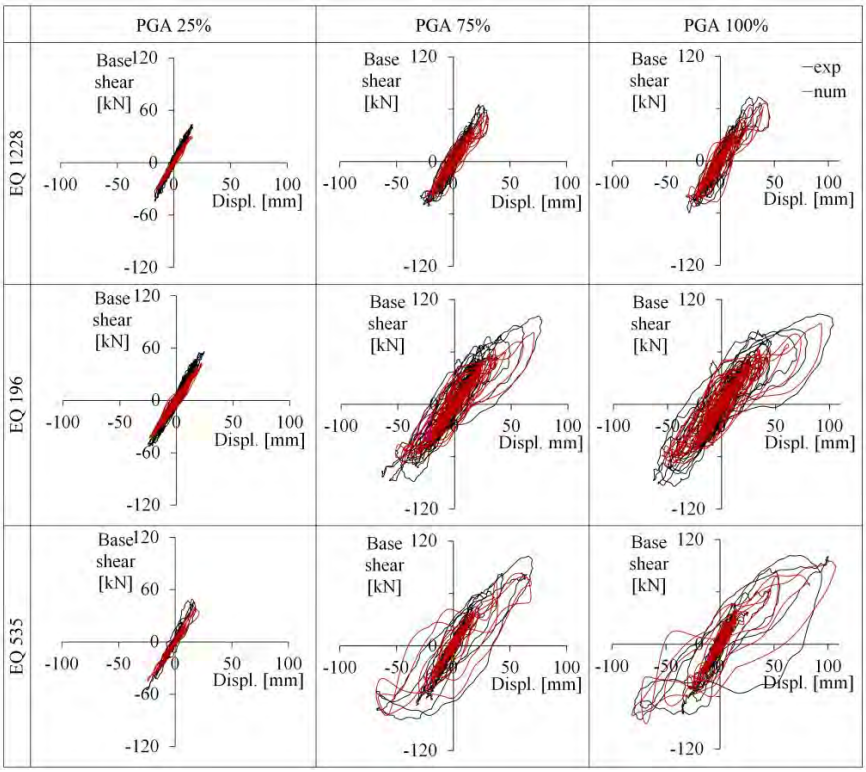

Figure 8: *Comparison between the global hysteretic response of the experimental and numerical braced model for earthquakes 1228, 196 and 535 at 25%, 75% and 100% of PGA , in terms of base shear vs top displacement.*

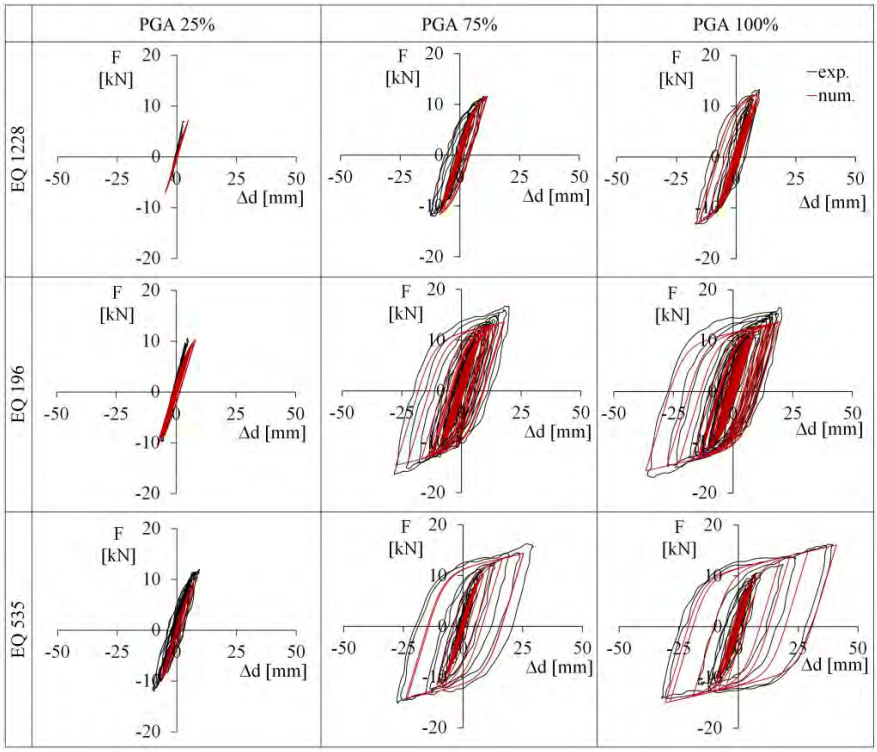

Figure 9: *Comparison between the experimental and numerical results of the local hysteretic response of UFP damper at the first storey of the bracing system for earthquakes 1228, 196 and 535 at 25%, 75% and 100% of PGA.*

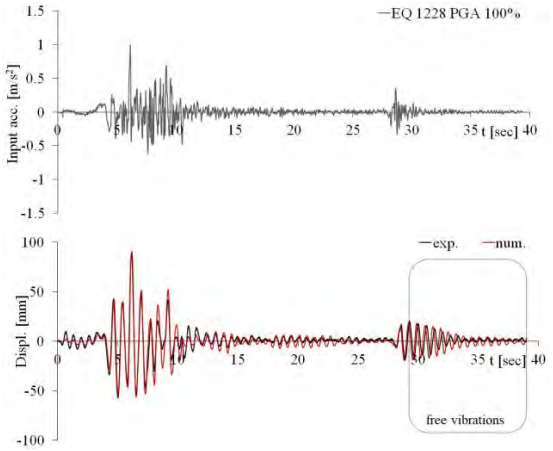

Figure 10: *Input acceleration and recorded top displacement of the bare post-tensioned frame model for earthquake 1228 at 100% of PGA.*

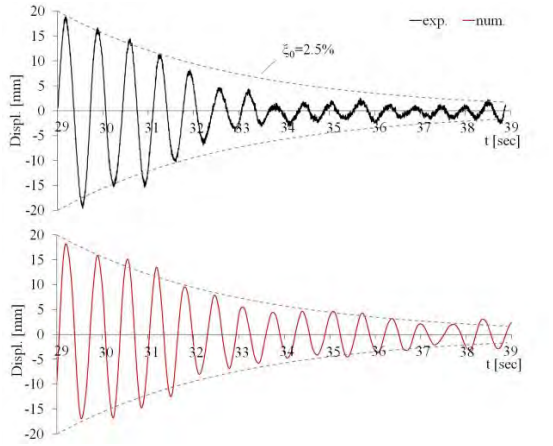

Figure 11: *Estimation of elastic damping from free vibration displacements versus time response for the bare post-tensioned frame model.*

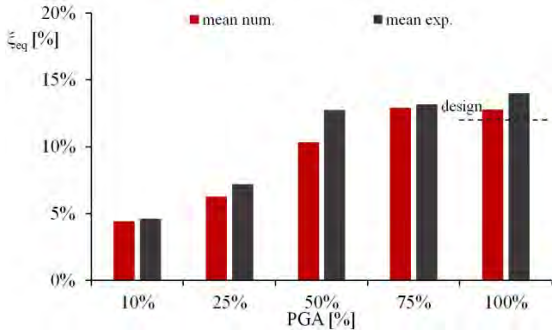

Figure 12: *Comparison between experimental and numerical estimation of equivalent damping of the post-tensioned timbre braced model.*

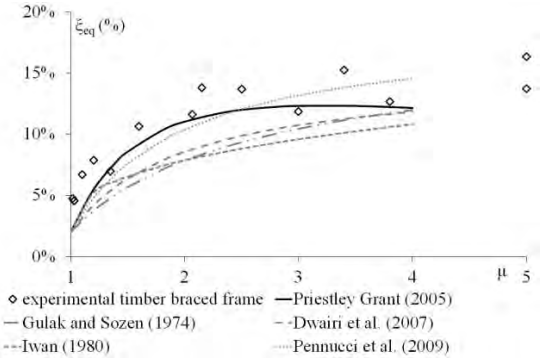

Figure 13: *Comparison between experimental estimation of equivalent damping and some of the existing equivalent damping formulations.*

5 CONCLUSIONS

This study estimates the experimental equivalent viscous damping of a post-tensioned timber framed model with dissipative bracing systems. Shaking table tests were performed at the structural laboratory of the University of Basilicata on a 3-D, 2/3 scaled, post-tensioned timber frame building in different configurations, with and without dissipative systems. The prototype model considered in this study was the Pres-Lam frame equipped with dissipative bracing systems, each composed by two V-inverted timber rods in series with two steel UFPs as dissipative dampers.

Non-linear dynamic analyses of the braced model were also conducted using 3 spectrum compatible earthquake ground motions at increasing PGA levels (from 10% to 100% of PGA). The results of the numerical time history analyses and experimental tests were in good agreement both in terms of global behaviour and local response of UFPs.

The experimental and numerical elastic damping contribution was estimated equal to 2.5% by applying the logarithmic decrement to the free vibration time-displacement response of the bare post-tensioned frame. Based on Jacobsen's formulation approach, the hysteretic damping contribution was estimated from the global numerical and experimental flag-shape hysteretic responses. The total equivalent damping of the braced post-tensioned model was estimated as sum of the two contribution, showing a good agreement between numerical and experimental results, with an increasing trend at lower PGA levels and it was stable around 13% and 14% at higher PGA levels. At the 100% of PGA (design level) the estimation of equivalent damping was in line with the design value of 12%.

Then, the experimental results were compared with some of the equations available in literature in terms of total equivalent viscous damping versus ductility. The results indicated that the DBD approach based on equation proposed by Priestley and Grant (2005) [11] for flag-shaped systems, was satisfactory for the post-tensioned braced frame considered in this study for the selected accelerograms, with some discrepancies at highest ductility.

ACKNOWLEDGEMENT

Authors would like to acknowledge the DPC-RELUIS 2019-2021 project for the financial support and Prof. Stefano Pampanin for his contribute to the research study.

REFERENCES

[1] Di Cesare, A., Ponzo, F.C., Vona, M., Dolce, M., Masi, A., Gallipoli, M.R., Mucciarelli, M. (2014). Identification of the structural model and analysis of the global seismic behaviour of a RC damaged building. *Soil Dynamics and Earthquake Engineering*, 65, 131-141

[2] Jacobsen, L. S. (1930). Steady forced vibrations as influenced by damping, *ASME Transactione* 52(1), 169–181.

[3] Jacobsen, L. S. (1960). Damping in composite structures. Proc., *2nd World Conf. on Earthquake Engineering*, Vol. 2, Science Council of Japan, Tokyo, 1029–1044.

[4] Rosenblueth, E., & Herrera, I. (1964). On a kind of hysteretic damping. *Journal of the Engineering Mechanics Division*, 90(4), 37-48.

[5] Gulkan, P., and Sozen, M. (1974). Inelastic response of reinforced concrete structures to earthquake motion. *ACI J.*, 71, 604–610.

[6] Iwan, W. D. (1980). Estimating inelastic response spectra from elastic spectra. *Earthquake Eng. Struct. Dyn.*, 8(4), 375–388.

[7] Chopra, Anil K. (1995). Dynamics of Structures: Theory and application to earthquake engineering Prentice Hall, USA

[8] Dwairi, H. M., Kowalsky, M. J., and Nau, J. M. (2007). Equivalent damping in support of direct displacement-based design. *J. Earthquake Eng.*, 11(4), 512–530.

[9] Filiatrault, A., Isoda, H., & Folz, B. (2003). Hysteretic damping of wood framed buildings. *Engineering Structures*, *25*(4), 461-471.

[10] Blandon, C. A., and Priestley, M. J. N. (2005). Equivalent viscous damping equations for direct displacement-based design. J. Earthquake Eng., 9(2), 257–278.

[11] Priestley, M. J. N., & Grant, D. N. (2005). Viscous damping in seismic design and analysis. Journal of earthquake engineering, 9(spec02), 229-255.

[12] Pennucci, D., Calvi, G. M., & Sullivan, T. J. (2009). Displacement-based design of precast walls with additional dampers. *Journal of Earthquake Engineering*, *13*(S1), 40-65.

[13] Bezabeh, M. A., Tesfamariam, S., & Stiemer, S. F. (2016). Equivalent viscous damping for steel moment-resisting frames with cross-laminated timber infill walls. *Journal of Structural Engineering*, *142*(1), 04015080.

[14] Priestley, M. J. N., Calvi, G. M., and Kowalsky, M. J. (2007). Displacement-Based Seismic Design of Structures. Pavia: IUSS Press, 670.

[15] Di Cesare, A., Ponzo, F.C. (2017). Seismic Retrofit of Reinforced Concrete Frame Buildings with Hysteretic Bracing Systems: Design Procedure and Behaviour Factor. Shock and Vibration, 2639361.

[16] Bianchi, S., Ciurlanti, J., & Pampanin, S. (2020). Comparison of traditional vs low-damage structural and non-structural building systems through a cost/performance-based evaluation. *Earthquake Spectra*, 8755293020952445.

[17] Priestley, N., Sritharan, S., Conley, J., and Pampanin, S. (1999). Preliminary results and conclusions, PRESSS five-story precast concrete test building. *PCI J.* 44, 42–67. doi: 10.15554/pcij.11011999.42.67

[18] Moroder, D., Smith, T., Dunbar, A., Pampanin, S., & Buchanan, A. (2018). Seismic testing of post-tensioned Pres-Lam core walls using cross laminated timber. *Engineering Structures*, 167, 639-654.

[19] Di Cesare, A., Ponzo, F.C., Nigro, D. (2014). Assessment of the performance of hysteretic energy dissipation bracing systems. *Bulletin of Earthquake Engineering*, 2014, 12(6), pp. 2777-2796

[20] Granello G., Palermo A., Pampanin S., Pei S., & van de Lindt J. (2020) Pres-Lam Buildings: State-of-the-Art., *Journal of Structural Engineering*, 146(6): 04020085. DOI: 10.1061/(ASCE)ST.1943-541X.0002603

[21] Di Cesare, A., Ponzo, F. C., Pampanin, S., Smith, T., Nigro, D., and Lamarucciola, N. (2019). Displacement based design of post-tensioned timber framed buildings with dissipative rocking mechanism. *Soil Dynamics and Earthquake Engineering*, 116, 317-330.

[22] Di Cesare, A., Ponzo, F. C., Lamarucciola, N., and Nigro, D. S. (2019). Seismic design and testing of post-tensioned timber buildings with dissipative bracing systems. *Frontiers in Built Environment*, 5, 104.

[23] Krawinkler, H., and Moncarz, P. D. (1981). Theory and Application of Experimental Model Analysis in Earthquake Engineering. Standford, CA: NASA STI/Recon Technical Report N 82.

[24] Di Cesare, A., Ponzo, F. C., Lamarucciola, N. and Nigro, D. (2020). Experimental seismic response of a resilient 3-storey post-tensioned timber framed building with dissipative braces. Bulletin of Earthquake Engineering. https://doi.org/10.1007/s10518-020-00969-y

[25] Ponzo, F. C., Di Cesare, A., Lamarucciola, N., & Nigro, D. (2019). Testing requirements of hysteretic energy dissipating devices according to Italian seismic code. *In: COMPDYN Proceedings*. vol. 2, p. 3323-3332, Crete, Greece, 24-26 June

[26] Di Cesare A., Ponzo F.C., Nigro D., Pampanin S., Smith T. (2017) Shaking table testing of post-tensioned timber frame building with passive energy dissipation systems. *Bulletin of Earthquake Engineering*, 15(10):4475-4498

[27] Computers and Structures Inc. 2014. SAP 2000 v. 16.1.0 [Software]. *Computers and Structures, Inc.*: Berkeley, CA.

[28] Ponzo, F. C., Di Cesare, A., Lamarucciola, N., Nigro, D., Pampanin, S., (2017). Modelling of post-tensioned timber-framed buildings with seismic rocking mechanism at the column-foundation connections. *Int. J. Comp. Meth. and Exp. Meas.*, Vol. 5, No. 6, 966–978.

[29] Di Cesare, A., Ponzo, F. C., Lamarucciola, N., and Nigro, D. (2019). Modelling of post-tensioned timber framed buildings with hysteretic bracing system: preliminary analysis. *In IOP Conference Series: Earth and Environmental Science* (Vol. 233, No. 2, p. 022026). IOP Publishing.
[30] Bouc, R. (1967) Forced vibration of mechanical system with hysteresis. *4th Conference on Nonlinear Oscillations*, Prague, CZ.
[31] Wen, Y. K. (1980) Equivalent linearization for hysteretic systems under random excitation. *Journal of Applied Mechanics*, 47(1): 150–154. https://doi.org/10.1115/1.3153594.
[32] Meirovitch, L. (2010). Fundamentals of vibrations. Waveland Press. ISBN 10: 1-57766-691-7